Self-calibration for Magnetic Resonance Fingerprinting

Self-calibration for Magnetic Resonance Fingerprinting

Roberto Duarte*, Audrey Repetti*†, and Yves Wiaux*
* Institute of Sensors, Signals and Systems, Heriot-Watt University, Edinburgh, EH14 4AS.
† Department of Actuarial Mathematics & Statistics, Heriot-Watt University, Edinburgh, EH14 4AS.

***Abstract*—In the context of quantitative Magnetic Resonance Imaging (qMRI), the recently proposed Magnetic Resonance Fingerprinting (MRF) technique has significantly reduced the acquisition time. MRF reconstructions are based on the correlation of multiple aggressively undersampled time acquisitions. Coil sensitivity calibration is a crucial step in the reconstruction process to obtain accurate results. Traditionally, MRF calibration is performed upstream of the imaging process, using a different acquisition. This technique makes the overall acquisition time consuming and may introduce artefacts in the image estimate. Usual MRI self-calibration methods, reconstructing independently the time acquisitions, are not suitable for highly undersampled MRF data. In this work, leveraging recent developments in non-convex optimisation, we propose the first self-calibration method for MRF, exploiting the correlation in the time acquisitions.**

I. Introduction

In MRF, the objective is to estimate the parameters associated with each of the N voxels of an imaged volume, from degraded undersampled measurements $\mathbf{Y} \in \mathbb{C}^{Q\times L\times C}$ [1]. These measurements are acquired from C coils, with an excitation sequence of length L. For each coil, and each excitation, Q degraded measurements are acquired. Let $\mathbf{M} \in \mathbb{C}^{N\times L}$ be the response of the imaged volume of interest. For every excitation $l \in \{1,\dots,L\}$ and coil $c \in \{1,\dots,C\}$, the corresponding observation $\mathbf{Y}_{:,l,c} \in \mathbb{C}^{Q}$ is given by $\mathbf{Y}_{:,l,c} = \mathbf{\Omega}_{:,:,l}\mathbf{F}\,\mathrm{Diag}(\mathbf{S}_{:,c})\mathbf{M}_{:,l} + \boldsymbol{\eta}_{:,l,c}$, where $\mathbf{\Omega} \in \{1,0\}^{Q\times N\times L}$ is the concatenation of L selection matrices, $\mathbf{F} \in \mathbb{C}^{N\times N}$ models the 2D discrete Fourier transform, $\mathbf{S} \in \mathbb{C}^{N\times C}$ is the concatenation of the C sensitivity maps, and Diag is a function that takes a vector and returns the corresponding diagonal matrix. Finally, $\boldsymbol{\eta} \in \mathbb{C}^{Q\times L\times C}$ is a realisation of a random i.i.d. Gaussian noise. Let $h\colon \mathbb{C}^{N\times C}\times\mathbb{C}^{N\times L} \to \mathbb{C}^{Q\times L\times C}$ be the linear mapping defining the complete acquisition process, i.e. $\mathbf{Y} = h(\mathbf{S},\mathbf{M}) + \boldsymbol{\eta}$. The image volume response $\mathbf{M}$ belongs to a non-convex set $\mathcal{B}$ that models the constraints from the physics of the magnetic resonance as well as other relevant phenomena such as the partial volume effect [1], [2]. The magnetisation sequence can be obtained by defining $\mathbf{M}$ as a minimiser of $F(\mathbf{S},\mathbf{M}) = 1/2\|\mathbf{Y} - h(\mathbf{S},\mathbf{M})\|_2^2$, under the constraint $\mathbf{M}\in\mathcal{B}$, when $\mathbf{S}$ is fixed and has been pre-calibrated.

Traditional MRF methods estimate $\mathbf{S}$ beforehand, using different acquisitions, making the data acquisition process more expensive. In addition, since calibration is performed by a single acquisition, $\mathbf{S}$ is calibrated up to a voxel-wise global phase. Whilst estimating $\mathbf{M}$ has been the focus of works such as [1], [2], the lack of advanced techniques for the coil sensitivity estimation can significantly affect the image reconstruction. Moreover, due to the highly undersampled MRF acquisitions, MRI self-calibration methods are not suitable. Hence the need for developing joint calibration and imaging methods for MRF. In the next section, we propose an optimisation approach to estimate simultaneously the sensitivity maps $\mathbf{S}$ and the image volume response $\mathbf{M}$.

II. Joint Calibration and Imaging for MRF

We propose to $\underset{\mathbf{M}\in\mathcal{B},\mathbf{S}\in\mathbb{R}^{N\times C}}{\text{minimise}}\ F(\mathbf{S},\mathbf{M})$. To solve this problem, we use an alternating forward-backward approach [3], described in Algorithm 1, where $\nabla_{\mathbf{M}}F$ (resp. $\nabla_{\mathbf{S}}F$) denotes the partial gradient of F with respect to $\mathbf{M}$ (resp. $\mathbf{S}$). Under technical conditions [3], the sequence $(\mathbf{M}^{(k)},\mathbf{S}^{(k)})_{k\in\mathbb{N}}$ generated by Algorithm 1 is guaranteed to converge to a critical point of the objective function of interest.

Algorithm 1 Joint Calibration and Imaging for MRF

Input: $\mathbf{S}^{(0)} \in \mathbb{C}^{N\times C}$, $\mathbf{M}^{(0)} \in \mathcal{B}$, $(I,J) \in \mathbb{N}_*^2$, $(\mu,\nu) \in (\mathbb{R}_*^+)^2$
for $k = 0, 1, \dots$ **do**
  $\widetilde{\mathbf{M}}^{(0)} = \mathbf{M}^{(k)}$ and $\widetilde{\mathbf{S}}^{(0)} = \mathbf{S}^{(k)}$
  for $i = 0, 1, \dots, I-1$ **do**
    $\mathbf{M}^{(i)} = \mathcal{P}_{\mathcal{B}}\left(\widetilde{\mathbf{M}}^{(i)} - \mu\nabla_{\mathbf{M}}F\left(\mathbf{S}^{(k)},\widetilde{\mathbf{M}}^{(i)}\right)\right)$
  end for
  $\mathbf{M}^{(k+1)} = \widetilde{\mathbf{M}}^{(I)}$
  for $j = 0, 1, \dots, J-1$ **do**
    $\mathbf{S}^{(j)} = \widetilde{\mathbf{S}}^{(j)} - \nu\nabla_{\mathbf{S}}F\left(\widetilde{\mathbf{S}}^{(j)},\mathbf{M}^{(k+1)}\right)$
  end for
  $\mathbf{S}^{(k+1)} = \widetilde{\mathbf{S}}^{(J)}$
end for

III. Results

We test our algorithm with a partial volume phantom using the model defined in [2]. As shown in Fig. 1, the estimated tissue proportion maps are close to the ground truth. While the algorithm is able to accurately estimate the parameters and the proportions of each tissue, the obtained proton densities are not accurate. This is due to the ambiguity in the operator h, i.e. for any voxel n, the norm of $\mathbf{M}_{n,:}$ can be absorbed in $\mathbf{S}_{n,:}$ and vice-versa. In future work, we aim to address the ambiguity by adding more prior information in the model such as, spatial regularisation on the proton density and smoothness in the sensitivity maps.

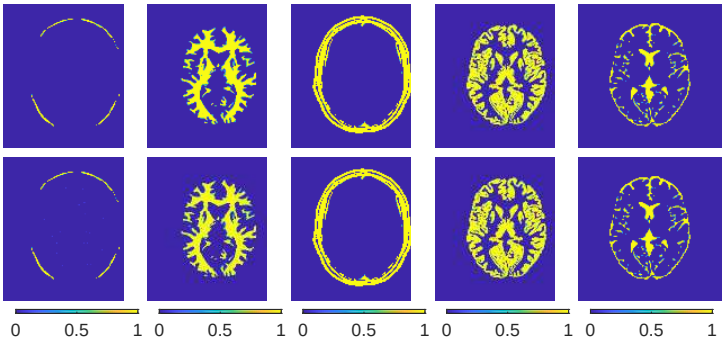

Fig. 1: Tissue proportion maps. The first row correspond to the Ground Truth and the second row to our reconstructions. The columns correspond, from left to right, to Adipose Tissue, White Matter, Muscle, Gray Matter and Cerebrospinal fluid.

References

[1] M. Davies, G. Puy, P. Vandergheynst, and Y. Wiaux, "A Compressed Sensing Framework for Magnetic Resonance Fingerprinting," *SIAM J. Imaging Sci.*, vol. 7, no. 4, p. 2623, Nov. 2014.
[2] R. Duarte, A. Repetti, P. A. Gómez, M. Davies, and Y. Wiaux, "Greedy approximate projection for magnetic resonance fingerprinting with partial volumes," Tech. Rep., 2018, https://arxiv.org/abs/1807.06912.
[3] E. Chouzenoux, J.-C. Pesquet, and A. Repetti, "A block coordinate variable metric forward-backward algorithm," *Journal of Global Optimization*, pp. 1–29, Feb. 2016.